

Transverse scattering and generalized Kerker effects in all-dielectric Mie-resonant meta-optics

Hadi K. Shamkhi¹, Kseniia V. Baryshnikova¹, Andrey Sayanskiy¹, Polina Kapitanova¹, Pavel D. Terekhov^{1,2,3,4}, Pavel Belov¹, Alina Karabchevsky^{1,2,3,4}, Andrey B. Evlyukhin^{1,5}, Yuri Kivshar^{1,6}, and Alexander S. Shalin¹

¹ITMO University, St. Petersburg 197101, Russia

²Electrooptics and Photonics Engineering Department, Ben-Gurion University, Beer-Sheva 8410501, Israel

³Ilse Katz Institute for Nanoscale Science & Technology, Ben-Gurion University, Beer-Sheva 8410501, Israel

⁴Center for Quantum Information Science and Technology, Ben-Gurion University, Beer-Sheva 8410501, Israel

⁵Laser Zentrum Hannover e.V., Hollerithallee, D-30419, Hannover, Germany and

⁶Nonlinear Physics Centre, Australian National University, Canberra ACT 2601, Australia

All-dielectric resonant nanophotonics has attracted a lot of attention recently due to the unique possibilities to control scattering of light in high-index dielectric nanoparticles and metasurfaces. One of the important concepts of dielectric nanophotonics is associated with the Kerker effect that drives the unidirectional scattering of light for nanoantennas and Huygens' metasurfaces. Here we suggest and demonstrate experimentally a novel effect manifested in the nearly complete *simultaneous suppression* of both forward and backward scattering fields. We extend this concept to dielectric metasurfaces that demonstrate zero reflection with transverse scattering and localization of light in the surface plane with the field enhancement for nonlinear and sensing applications.

Introduction. Light scattering by subwavelength particles is closely associated with optically-induced multipolar response. Co-existence of magnetic and electric dipolar resonances makes it possible to achieve either constructive or destructive interference leading to remarkable scattering properties of subwavelength dielectric particles [1–3]. In particular, strong forward-to-backwards asymmetric scattering (often termed as the Kerker effect) is achieved as a result of interfering electric and magnetic dipole modes [4–6], or quadrupolar modes with appropriate phase relations [3, 7–9]. Overlapping electric and magnetic multipoles of higher orders opens a way for novel strategies for the effective shaping of light beyond the conventional forward and backward directions [2, 3]. For example, an isolated V-shaped plasmonic nanoantenna [10] or a nanoparticle trimer [11] have been suggested for achieving side-directed scattering through breaking of scatterer's symmetry. Moreover, the conditions for the simultaneous cancellation of both forward and backward scattering have been obtained in the quasi-static approximation for a special case of radially anisotropic particles [12]. However, for satisfying the power conservation requirements and suppressing the forward scattering at the same time, the suggested particles should possess a gain.

Semiconductor materials such as silicon possess a relatively large values of dielectric permittivity in the visible frequency range allowing to excite multipole resonances of different orders in subwavelength particles. In addition, such materials possess rather low losses [1, 10, 13, 14], and they are commonly employed as materials for all-dielectric nanoantennas [6], metadevices [15, 16], and metasurfaces [17, 18]. Here we predict and demonstrate a new effect in high-index Mie-resonant nanophotonics characterized by the transverse scattering by subwavelength particles with the simultaneous suppression of both forward and backward scattering fields.

We consider a subwavelength silicon particle of the simplest form (a sphere or a cube) without any additional requirements [10, 12]. For the first time to our knowledge, we derive the essential conditions for the multipoles of the scattering

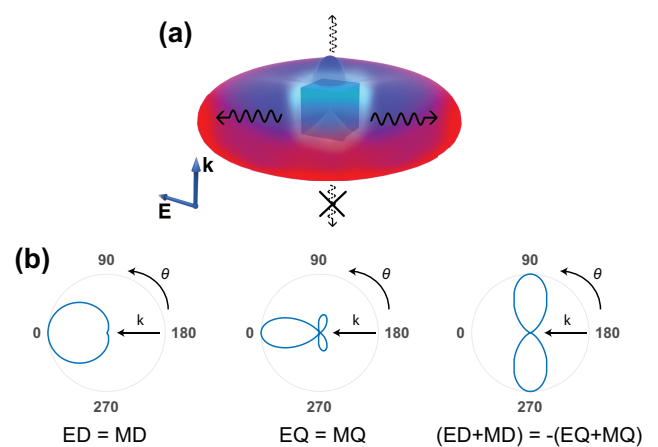


FIG. 1: (a) Transverse scattering pattern for a cubic nanoparticle. Small forward scattering corresponds to a contribution of higher-order multipoles in accord with the optical theorem. (b) Concept of the formation of an ideal transverse scattering pattern. Electric dipole (ED) is in-phase with a magnetic dipole (MD) and an electric quadrupole (EQ) is in-phase with a magnetic quadrupole (MQ), while the dipoles are out-of-phase with the quadrupoles.

fields to support the lateral-only scattering pattern depending on the optical properties of a substrate. We present the results of the proof-of-principle microwave experiments and demonstrate a nearly perfect agreement with our analytical (based on the Mie theory [19]) and numerical (based on the COMSOL Multiphysics [20]) results. The transverse scattering appears to follow a strong near-field localization inside the particles being conceptually similar to the recently found optical anapole states [21, 22]. Both these effects are of a high demand for a variety of linear and nonlinear applications including four-wave mixing [23] and all-optical light modulation [24].

Concept. We start with the Cartesian multipole decomposition of the field scattered by an arbitrary subwavelength particle. The surrounding medium is a free space with relative permittivity $\epsilon = 1$. The incident wave is assumed to be lin-

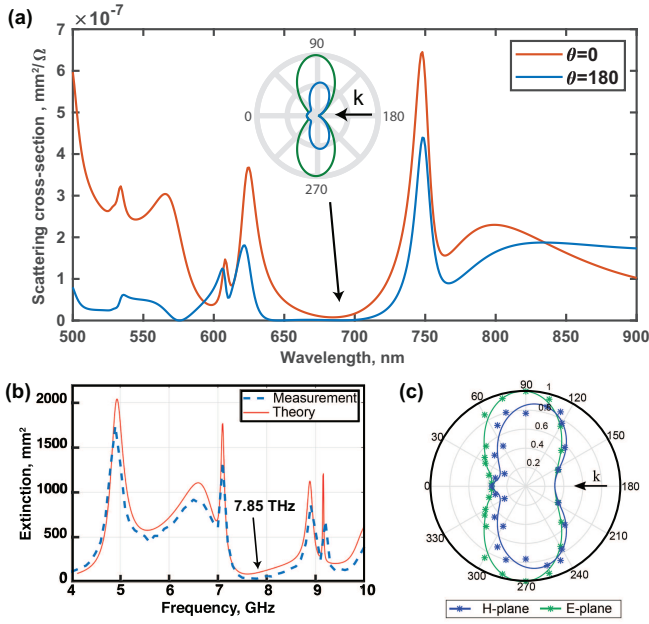


FIG. 2: (a) Forward ($\theta=0$) and backward ($\theta=180^\circ$) scattering cross-sections calculated for a silicon sphere of 140 nm radius in free space. The inset referring to 685 nm is the corresponding transverse scattering patterns: the green (blue) line corresponds to the plane of the incident electric (magnetic) field polarization. (b,c) Experimental results. (b) Comparison of the extinction cross-section calculated with the Mie theory and measured experimentally. (c) Scattering patterns at the frequency $f = 7.85$ GHz, where the green (blue) curve corresponds to the plane of the incident electric (magnetic) fields polarization. Results are obtained for a ceramic sphere with dielectric permittivity $16+0.001i$ and radius 7.5 mm, respectively.

early polarized along z -axis: $\mathbf{E}_{inc} = E_0 e^{ikz} \mathbf{x}$, where k is the wavenumber. The exact pattern of the angular distribution of the total scattered light is defined by a superposition of multipoles, and it has the following form (up to the quadrupole terms) [25],

$$\begin{aligned} \mathbf{E}_{sca}(\mathbf{n}) \cong & \frac{k^2 e^{ikr}}{4\pi r \epsilon_0} \left(\mathbf{n} \times [\mathbf{p} \times \mathbf{n}] + \frac{1}{c} [\mathbf{m} \times \mathbf{n}] \right. \\ & \left. + \frac{ik}{6} [\mathbf{n} \times [\mathbf{n} \times (\overleftrightarrow{Q} \cdot \mathbf{n})]] + \frac{ik}{2c} [\mathbf{n} \times (\overleftrightarrow{M} \cdot \mathbf{n})] \right), \end{aligned} \quad (1)$$

where $\mathbf{n} = \mathbf{r}/r$ is the unit vector directed from particle's center towards an observation point; c is the speed of light, $\mathbf{p}(\mathbf{m})$, $\overleftrightarrow{Q}(\overleftrightarrow{M})$ are the electric (magnetic) dipole and electric (magnetic) quadrupole, respectively.

From Eq. (1), one can derive the conditions for the simultaneous suppression of scattering in both forward and backward directions. We derive them analytically and compare with numerical results for a high-index silicon sphere in the visible frequency range. To do so, we define the angular distribution of the total differential scattering cross-section, up to

the dipole and quadrupole terms [26]:

$$\begin{aligned} \frac{d\sigma^T}{d\Omega}(\theta) = & \left| \left(\frac{\alpha_p}{\epsilon_0} + \frac{k^2 \alpha_Q}{4 \cdot 3\epsilon_0} \cos \theta + \frac{1}{\epsilon_0} \sum_{j \neq p, Q} A_j^E(k, \theta) \alpha_j \right) \right. \\ & \left. + \left(\alpha_m \cos \theta + \frac{k^2}{4} \alpha_M \cos 2\theta + \sum_{j \neq m, M} A_j^H(k, \theta) \alpha_j \right) \right|^2, \end{aligned} \quad (2)$$

where θ is the polar angle, and the power distribution is considered to be symmetrical in the azimuthal angle plane. The terms A_j^E and A_j^H represent the contributions of higher-order multipoles [26, 27]. The scattering is characterized by the electric and magnetic dipolar (α_p , α_m) and quadrupolar (α_Q , α_M) polarizabilities, respectively. We derive the particle polarizabilities by comparing the Mie theory expansion with the scattering from a particle illuminated by a plane wave in Eq. (1) [27]. The induced multipole moments could be expressed as the following [26]:

$$\begin{aligned} \mathbf{p} &= \alpha_p \mathbf{E}_{inc}; \quad \mathbf{m} = \alpha_m \mathbf{H}_{inc}; \quad Q = \alpha_Q \frac{\nabla \mathbf{E}_{inc} + (\nabla \mathbf{E}_{inc})^T}{2}; \\ M &= \alpha_M \frac{\nabla \mathbf{H}_{inc} + (\nabla \mathbf{H}_{inc})^T}{2}. \end{aligned} \quad (3)$$

Now we calculate the corresponding contributions to the differential scattering cross-section neglecting higher-order terms A_j^E and A_j^H . As a matter of fact, it is possible to find a particle with negligible contribution of higher-order multipoles [2]. Then, Eq. (2) takes the following form:

$$\begin{aligned} \frac{d\sigma}{d\Omega}(\theta) = & \frac{k^4}{(4\pi)^2} \left(\left| \frac{\alpha_p}{\epsilon_0} \right|^2 + |\alpha_m|^2 \cos^2 \theta + \frac{k^4}{16} \left| \frac{\alpha_Q}{3\epsilon_0} \right|^2 \cos^2 \theta \right. \\ & \left. + \frac{k^4}{16} |\alpha_M|^2 \cos^2 2\theta + \frac{2}{\epsilon_0} \text{Re}\{\alpha_p \alpha_m\} \cos \theta \right. \\ & \left. + \frac{k^4}{24\epsilon_0} \text{Re}\{\alpha_Q \alpha_M\} \cos \theta \cos 2\theta \right). \end{aligned} \quad (4)$$

Coherent contribution of the electric and magnetic dipoles make the radiation pattern to be directed mainly in the forward or backward half spaces depending on whether the term $\text{Re}\{\alpha_p \alpha_m\}$ is positive or negative, respectively [5]. We notice that α_p and α_m are complex values and the equality $\epsilon_0 \alpha_m / \alpha_p$ becomes real only if the dipoles are in-phase or out-of-phase. To obtain the total suppression of the backward scattering ($|\theta| \geq 90^\circ$) (see Figure 1), the dipoles are to be in-phase and have the same polarizabilities; for suppression of the forward scattering ($|\theta| \leq 90^\circ$) the dipoles must also have the same polarizabilities, however the phase has to be shifted by π (antiphase case). These cases are known as the Kerker and anti-Kerker conditions [28], the former can be formulated as

$$|\alpha_p / \epsilon_0| = |\alpha_m|, \quad \arg(\alpha_p) = \arg(\alpha_m) + 2\pi n, \quad (5)$$

where n is integer.

For the electric and magnetic quadrupoles only, similar to the case of the dipoles, the equality $\alpha_Q / 3\epsilon_0 \alpha_M$ becomes real only when the complex magnitudes of α_Q and $3\epsilon_0 \alpha_M$

are either in-phase or out-of-phase, and they can be called "quadrupolar Kerker-like conditions",

$$|\alpha_Q| = |3\epsilon_0\alpha_M|, \quad \arg(\alpha_Q) = \arg(\alpha_M) + 2\pi n, \quad (6)$$

where n is an integer. We consider the total scattering in the upper and lower half spaces (see Eq. (2)). Obviously, it is governed by the coupling terms $R(\alpha_p\alpha_m)$, $R(\alpha_Q\alpha_M)$, and $R((\alpha_p/\epsilon_0 + \alpha_m)[\alpha_Q/(3\epsilon_0) + \alpha_M])$. The simultaneous application of the obtained conditions (5) and (6) to the dipole and quadrupole unidirectional scattering leads to the two possible scattering patterns depending on the phase relation between dipoles and quadrupoles,

$$\arg\left(\frac{\alpha_p}{\epsilon_0} + \alpha_m\right) = \pm \arg\left(\frac{\alpha_Q}{3\epsilon_0} + \alpha_M\right). \quad (7)$$

The first condition (with the sign plus) corresponds to the constructive interference of the dipoles and quadrupoles scattered forward and making the unidirectional scattering stronger.

Generally speaking, the multipolar coupling enhances the field directionality, and it lays a key role for the suppression of the backward scattering [7]. We can generalise the conditions (5)-(7) to the whole set of multipoles, and it could be referred to as the generalized Kerker condition,

$$\frac{d\sigma^T}{d\Omega}(\theta = 0^\circ) = 0. \quad (8)$$

The second scattering regime described by Eq. (7) (with the sign minus) corresponds to the case, when both forward and backward scattering are suppressed due to destructive interference between the combined coherent dipoles and combined coherent quadrupoles in the forward direction. In addition to the condition (8), the dipole-quadrupole interaction (5)-(7) also satisfy

$$\frac{d\sigma^T}{d\Omega}(\theta = 180^\circ) \cong 0. \quad (9)$$

Unlike the generalized Kerker conditions, this kind of interaction leads to the formation of a transverse scattering pattern as shown in Figure 1. The side lobes of the quadrupoles form a scattering pattern in the lateral plane. However, for subwavelength particles it is impossible to achieve such patterns because of the optical theorem that links the total extinction cross-section of a particle with the forward scattered fields. Therefore, the forward scattering cannot be completely eliminated, but it can be suppressed significantly provided the conditions (5)-(9) are satisfied. Figure 1(b) shows schematically our concept of the collective interferences of dipole and quadrupole moments.

The differential scattering cross-sections (the energy scattered either in the forward or backward directions) for a spherical Si particle of 140 nm radius are shown in Fig. 2(a). The conditions (6)-(7) are almost satisfied at the wavelength of 685 nm, when the backward intensity vanishes while the forward intensity reaches its minimum.

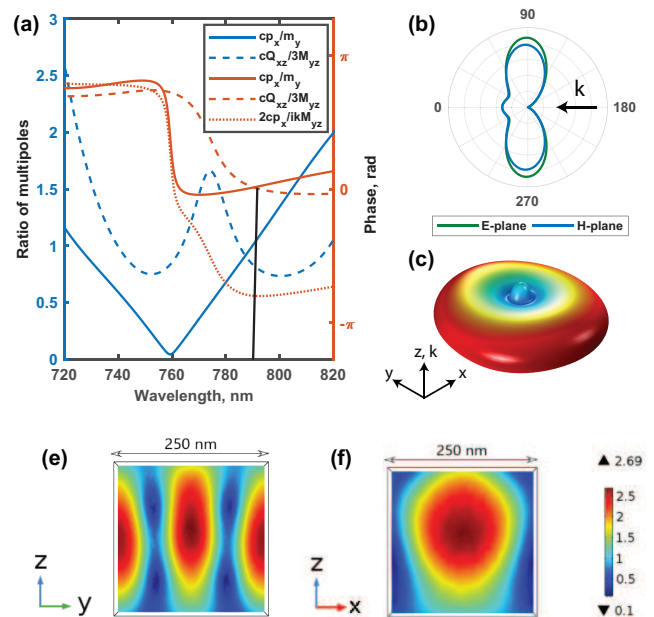


FIG. 3: (a) Amplitudes and phases of the multipole ratios from Eq. (10) for a cubic Si nanoparticle with the edge of 250 nm. The black vertical line shows the wavelength corresponding to the transverse scattering $\lambda=788$ nm. (b,c) Two- and three-dimensional scattering patterns at $\lambda=788$ nm. (e,f) Calculated electric field inside the nanoparticle with the transverse scattering pattern, $\lambda = 788$ nm in the xy and xz planes, respectively.

Experimental results. Based on scalability of Maxwell's equations, we verify our concept by measuring the extinction cross-section and scattering patterns of a spherical particle in the microwave frequency range. To mimic the scattering properties of a silicon nanoparticles at microwaves, we use MgO-TiO₂ ceramic spheres characterized by the dielectric constant $\epsilon = 16$ and dielectric loss factor of about 0.00112, measured in the range 9-12 GHz [29]. A spherical particle with the radius $a=7.5$ mm is located in a microwave chamber for the measurements in the frequency range 4-10 GHz. To approximate a plane wave excitation, we employ a rectangular horn antenna (TRIM 0.75-18 GHz; DR) connected to the transmitting port of a vector network analyzer (Agilent E8362C). The ceramic sphere is located in the far-field of the antenna, at a distance of approximately 2.5 m, and the second horn antenna (TRIM 0.75 - 18 GHz; DR) is used as a receiver to observe the transmitted signal. Forward scattering is obtained from the transmission coefficient. The total extinction cross-section is extracted from the measured complex magnitude of the forward scattered signal by means of the optical theorem [30]. The measured extinction is compared with the theoretically obtained results (Mie theory) in Fig. 2(b). To measure the two-dimensional scattering diagram the experimental setup is slightly changed. The transmitting antenna and the ceramic sphere are fixed, whereas the receiving antenna moves around the spherical particle in the xz plane. The scattering cross-section patterns for both theoretical (Mie the-

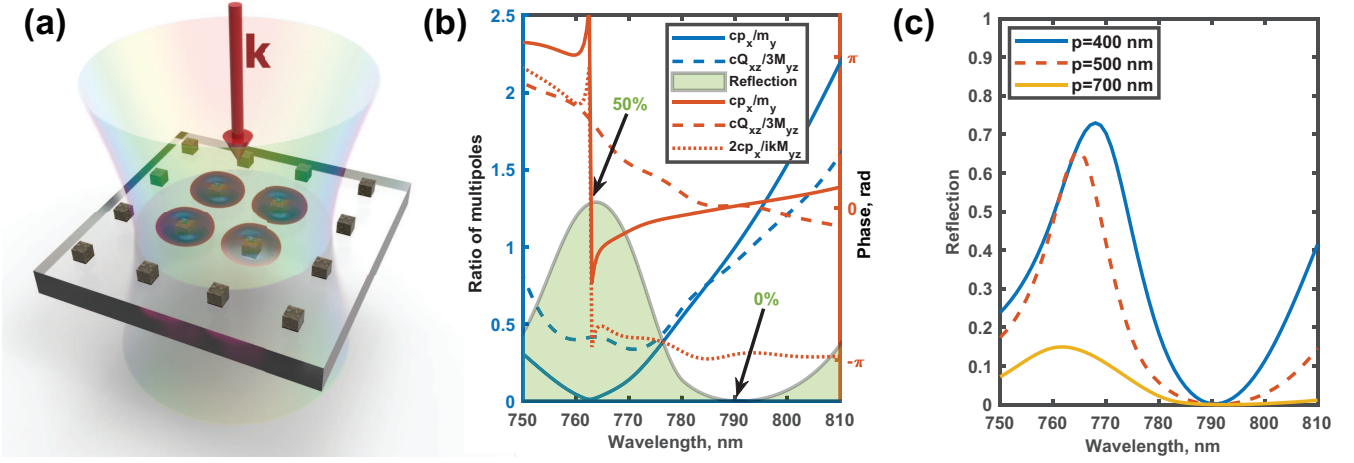


FIG. 4: (a) Schematics of a metasurface created by a lattice of cubic nanoparticles realizing strong transversal scattering. (b) Ratios and phases of the multipoles defined by Eq. (10) for a cube with the edge of 250 nm and the period $p = 500$ nm, and the corresponding reflection coefficient (the gray curve filled with green). (c) Reflection coefficient from a square lattice of Si nanocubes with the periods: $p = 400$ nm, 500 nm, and 700 nm, respectively.

ory) and measured data in the xz plane are shown in Fig. 2(c). We observe the lateral scattering to occur for the broadband off-resonance region from $f = 7.6$ GHz to $f = 7.9$ GHz.

Nonspherical nanoparticles. Next, we extend our results to a more general case of nonspherical particles by employing the Cartesian multipole moments [2, 31], and for simplicity select cubic particles.

Under a plane wave illumination, the Cartesian multipoles could be reduced to some nonzero components as $\mathbf{p} = p_x \mathbf{x}$, $\mathbf{m} = m_y \mathbf{y}$, $\hat{Q} = Q_{xz}(\mathbf{xz} + \mathbf{zx})$, and $\hat{M} = M_{yz}(\mathbf{yz} + \mathbf{zy})$. After applying the procedure similar to above, the conditions for the transverse scattering can be written in the form:

$$cp_x/m_y = 1; cQ_{xz}/3M_{yz} = 1; 2cp_x/ikM_{yz} = -1. \quad (10)$$

As an example, we consider silicon cubic nanoparticles. Figure 3(a) shows the calculated absolute values of the ratios from Eq. (10) and their phases being the phase differences between the involved multipoles. At the target wavelength $\lambda = 788$ nm (black vertical line), one can see that the dipoles are in-phase (red solid line) with the nearly equal amplitudes (blue solid line) indicating the Kerker effect. The quadrupoles, on the other hand, have comparable values and $cQ_{xz}/3M_{yz} = 0.94$ (blue dashed curve) and are in phase (red dashed curve), which explains the generalized Kerker effect under the assumption that higher multipoles are negligible. The phase difference between the coherent dipoles and quadrupoles (red dotted line) is about 0.75π . The corresponding scattering patterns are shown in Figs. 3(b,c). Hence, there is the almost complete scattering suppression in the forward and backward directions. However, the suppression of the forward scattering is not complete owing to the optical theorem. In Figs. 3(e,f) we demonstrate the electric near-field in both yz and xz planes inside the cubic nanoparticle at the wavelength of the transverse scattering. The observed near-field enhancement is accompanied by the strong scattering suppress-

ion resembling the case of the anapole mode where the dipole radiation is almost cancelled by that of the electric toroidal moment. This effect of the localization of light could be of a great interest for nonlinear applications.

it Metasurfaces. Finally, we study metasurfaces composed of cubic nanoparticles, which allow to satisfy the condition (10) for the transverse scattering in the visible range. Figure 5(a) shows schematically a square lattice of identical cubic nanoparticles illuminated with a normally incident plane wave. In the far-field region, the reflection is determined by the effective polarizabilities and multipole moments of a central nanoparticle [32] taking into account the interaction with all other nanoparticles in the metasurface. However, this interaction appears to be rather weak even for the lattice spacing less than the wavelength for silicon nanoparticles [33], which allows us to suggest that the obtained conditions (10) will hold.

We have performed full-wave numerical simulations of metasurfaces with the lattice spacings 400 nm, 500 nm, and 700 nm. Figure 5(b) shows the ratios of multipoles (10) obtained for an isolated particle (see Fig. 3). Since the cube polarizabilities are affected by coupling, the multipole moments of the nanocube within the array still satisfies the transverse scattering pattern conditions (10). In the wavelength range 787-793 nm, the coherent dipoles are nearly in-phase (red solid curve), quadrupoles are in-phase too (red dashed curve), but they are in anti-phase with each other (red dotted curve). With the close to unity amplitude ratios (blue solid and dashed curves), the metasurface shows a nearly perfect simultaneous forward and backward scattering suppression, similar to an isolated nanoparticle (see Fig. 3). Therefore, in this wavelength range, the metasurface reflection vanishes [see the background green area in Fig. 5(b)], despite the fact that the light interacts with the structure generating slightly different multipole moments. In contrast to the well-known

Huygens' metasurfaces [18], the novel metasurfaces introduced here suppress almost completely the scattering in the forward direction being nearly invisible.

Also, we analyze the effect of the lattice spacing on optical properties of the metasurface. Figure 5(c) shows that all resonance change their spectral positions and amplitudes, and the zero-reflection region broadens with increasing the inter-particle distance.

In conclusion, we have uncovered a novel effect of the transverse scattering of light by high-index subwavelength particles of different shapes with the simultaneous suppression of both forward and backward scattering. This unusual effect occurs when in-phase electric and magnetic dipoles become out of phase with the corresponding quadrupoles. Employing the Mie theory, we have obtained the conditions for the simultaneous suppression of scattering in both forward and backward directions, and have employed the multipole expansion to generalize the conditions for arbitrary subwavelength particles. Experimental data for the microwave spectral range have proven the concept for a ceramic sphere in a free space with a good agreement between theoretical and experimental results. Finally, we have studied metasurfaces consisting of nanoparticles with the transverse scattering patterns and demonstrated periodicity-dependent zero reflection of such metasurfaces. In contrast to Huygens metasurfaces, the considered metasurfaces scatter neither forward nor backward being almost invisible for incident light. These effects can be employed for efficient beam splitting and switching, as well as strong field enhancement for nonlinear interactions and sensing.

The authors acknowledge a financial support from the Russian Fund for Basic Research (grants 18-02-00414, 18-52-00005); the Ministry of Education and Science of the Russian Federation (grant 3.4982.2017/6.7), the Strategic Fund of the Australian National University, and the Australian Research Council. Calculations of multipole moments and scattering patterns have been supported by the Russian Science Foundation (grant 16-12-10287). Experimental characterization of ceramic particles has been supported by the Russian Science Foundation (grant 17-19-01731). YK thanks Dr. Wei Liu for useful discussions and suggestions.

[1] S. Kruk and Y. Kivshar, *Functional meta-optics and nanophotonics governed by Mie resonances*, ACS Photonics **4**, 2638 (2017).
 [2] P.D. Terekhov, K. V Baryshnikova, Y.A. Artemyev, A. Karabchevsky, A.S. Shalin, and A.B. Evlyukhin, *Multipolar response of nonspherical silicon nanoparticles in the visible and near-infrared spectral ranges*, Phys. Rev. B **96**, 35443 (2017).
 [3] W. Liu and Y.S. Kivshar, *Generalized Kerker effects in nanophotonics and meta-optics*, Opt. Express **26**, 13085 (2018).
 [4] M. Kerker, D.-S. Wang, and C.L. Giles, *Electromagnetic scattering by magnetic spheres*, J. Opt. Soc. Am. **73**, 765 (1983).
 [5] M. Nieto-Vesperinas, R. Gomez-Medina, and J.J. Saenz, *Angle-*

suppressed scattering and optical forces on submicrometer dielectric particles, J. Opt. Soc. Am. A **28**, 54 (2011).
 [6] A.E. Krasnok, A.E. Miroshnichenko, P.A. Belov, and Y.S. Kivshar, *Huygens' optical elements and YagiUda nanoantennas based on dielectric nanoparticles*, JETP Letters **94**, 593 (2011).
 [7] W. Liu, J. Zhang, B. Lei, H. Ma, W. Xie, and H. Hu, *Ultra-directional forward scattering by individual core-shell nanoparticles*, Opt. Express **22**, 16178 (2014).
 [8] A.E. Krasnok, C.R. Simovski, P.A. Belov, and Y.S. Kivshar, *Superdirective dielectric nanoantennas*, Nanoscale **6**, 7354 (2014).
 [9] A. Pors, S.K.H. Andersen, and S.I. Bozhevolnyi, *Unidirectional scattering by nanoparticles near substrates: generalized Kerker conditions*, Opt. Express **23**, 28808 (2015).
 [10] J. Li, N. Verellen, D. Vercruyse, T. Bearda, L. Lagae, and P. Van Dorpe, *All-dielectric antenna wavelength router with bidirectional scattering of visible light*, Nano Lett. **16**, 4396 (2016).
 [11] G. Lu, Y. Wang, R.Y. Chou, H. Shen, Y. He, Y. Cheng, and Q. Gong, *Directional side scattering of light by a single plasmonic trimer*, Laser & Photonics Rev. **9**, 530 (2015).
 [12] Y.X. Ni, L. Gao, A.E. Miroshnichenko, and C.W. Qiu, *Controlling light scattering and polarization by spherical particles with radial anisotropy*, Opt. Express **21**, 8091 (2013).
 [13] A.I. Kuznetsov, A.E. Miroshnichenko, Y.H. Fu, J. Zhang, and B. Lukyanchuk, *Magnetic light*, Sci. Rep. **2**, 492 (2012).
 [14] A.B. Evlyukhin, S.M. Novikov, U. Zywietz, R.L. Eriksen, C. Reinhardt, S.I. Bozhevolnyi, and B.N. Chichkov, *Demonstration of magnetic dipole resonances of dielectric nanospheres in the visible region*, Nano Lett. **12**, 3749 (2012).
 [15] S. Kruk, B. Hopkins, I.I. Kravchenko, A. Miroshnichenko, D.N. Neshev, and Y.S. Kivshar, *Broadband highly efficient dielectric metadevices for polarization control*, APL Photonics **1**, 30801 (2016).
 [16] P. Genevet, F. Capasso, F. Aieta, M. Khorasaninejad, and R. Devlin, *Recent advances in planar optics: from plasmonic to dielectric metasurfaces*, Optica **4**, 139 (2017).
 [17] I. Staude, A.E. Miroshnichenko, M. Decker, N.T. Fofang, S. Liu, E. Gonzales, J. Dominguez, T.S. Luk, D.N. Neshev, I. Brener, and Y. Kivshar, *Tailoring directional scattering through magnetic and electric resonances in subwavelength silicon nanodisks*, ACS Nano **7**, 7824 (2013).
 [18] M. Decker, I. Staude, M. Falkner, J. Dominguez, D.N. Neshev, I. Brener, T. Pertsch, and Y.S. Kivshar, *High-efficiency dielectric Huygens surfaces*, Adv. Opt. Mater. **3**, 813 (2015).
 [19] D.R. Bohren, C. F. Huffman, *Absorption and Scattering of Light by Small Particles* (Wiley, New York, 1983).
 [20] COMSOL Multiphysics, www.comsol.com (Stockholm, Sweden).
 [21] A.A. Basharin, V. Chuguevsky, N. Volsky, M. Kafesaki, and E.N. Economou, *Extremely high Q-factor metamaterials due to anapole excitation*, Phys. Rev. B **95**, 35104 (2017).
 [22] A.E. Miroshnichenko, A.B. Evlyukhin, Y.F. Yu, R.M. Bakker, A. Chipouline, A.I. Kuznetsov, B. Lukyanchuk, B.N. Chichkov, and Y.S. Kivshar, *Nonradiating anapole modes in dielectric nanoparticles*, Nat. Commun. **6**, 8069 (2015).
 [23] Y. Zhang and Y. Wang, *Nonlinear optical properties of metal nanoparticles: a review*, RSC Adv. **7**, 45129 (2017).
 [24] Y. Yang, W. Wang, A. Boulesbaa, I.I. Kravchenko, D.P. Briggs, A. Poretzky, D. Geoghegan, and J. Valentine, *Nonlinear Fano-resonant dielectric Metasurfaces*, Nano Lett. **15**, 7388 (2015).
 [25] A.B. Evlyukhin, T. Fischer, C. Reinhardt, and B. Chichkov, *Optical theorem and multipole scattering of light by arbitrarily shaped nanoparticles*, Phys. Rev. B **94**, 205434 (2016).
 [26] J.D. Jackson, *Classical Electrodynamics*, 3rd edition (Wiley,

- New York, 1998).
- [27] 31 A. Alú and N. Engheta, *Guided propagation along quadrupolar chains of plasmonic nanoparticles*, Phys. Rev. B **79**, 235412 (2009).
- [28] R. Gomez-Medina, B. Garcia-Camara, I. Suarez-Lacalle, F. Gonzalez, F. Moreno, M. Nieto-Vesperinas, and J.J. Saenz, *Electric and magnetic dipolar response of germanium nanospheres: interference effects, scattering anisotropy, and optical forces*, J. Nanophotonics **5**, 53510 (2011).
- [29] A. Kanareykin, W. Gai, J.G. Power, E. Nenasheva, and A. Altmark, *Transformer ratio enhancement experiment*, Proc. 2003 Part. Accel. Conf. (2003), pp. 18941896.
- [30] R.G. Newton, *Optical theorem and beyond*, Am. J. Phys. **44**, 639 (1976).
- [31] R.E. Raab and O.L. De Lange, *Multipole Theory in Electromagnetism: Classical, Quantum, and Symmetry Aspects, with Applications* (Oxford University Press, 2005).
- [32] V.E. Babicheva and A.B. Evlyukhin, *Metasurfaces with electric quadrupole and magnetic dipole resonant coupling*, ACS Photonics **5**, 2022 (2018).
- [33] A.B. Evlyukhin, C. Reinhardt, A. Seidel, B.S. Lukyanchuk, and B.N. Chichkov, *Optical response features of Si-nanoparticle arrays*, Phys. Rev. B **82**, 1 (2010).